Investigation of Cephalexin Removal Using Biochar Derived from *Nephelium lappaceum* Seeds

Varatharajan Varalakshmi[1], Velusamy Karthik[2*], Periyasamy Selvakumar[3], Perumal Muthumari [1]

[1]*Department of Biotechnology, P.S.R Engineering College, Sivakasi, Tamilnadu, India*

[2]*Department of Industrial Biotechnology, Government College of Technology, Coimbatore, Tamilnadu, India*

[3]*Department of Chemical Engineering, School of Mechanical, Chemical and Materials Engineering, Adama Science and Technology University, Adama, 1888, Ethiopia*

Corresponding Author's Email: karthik.v.ibt@gct.ac.in

GRAPHICAL ABSTRACT

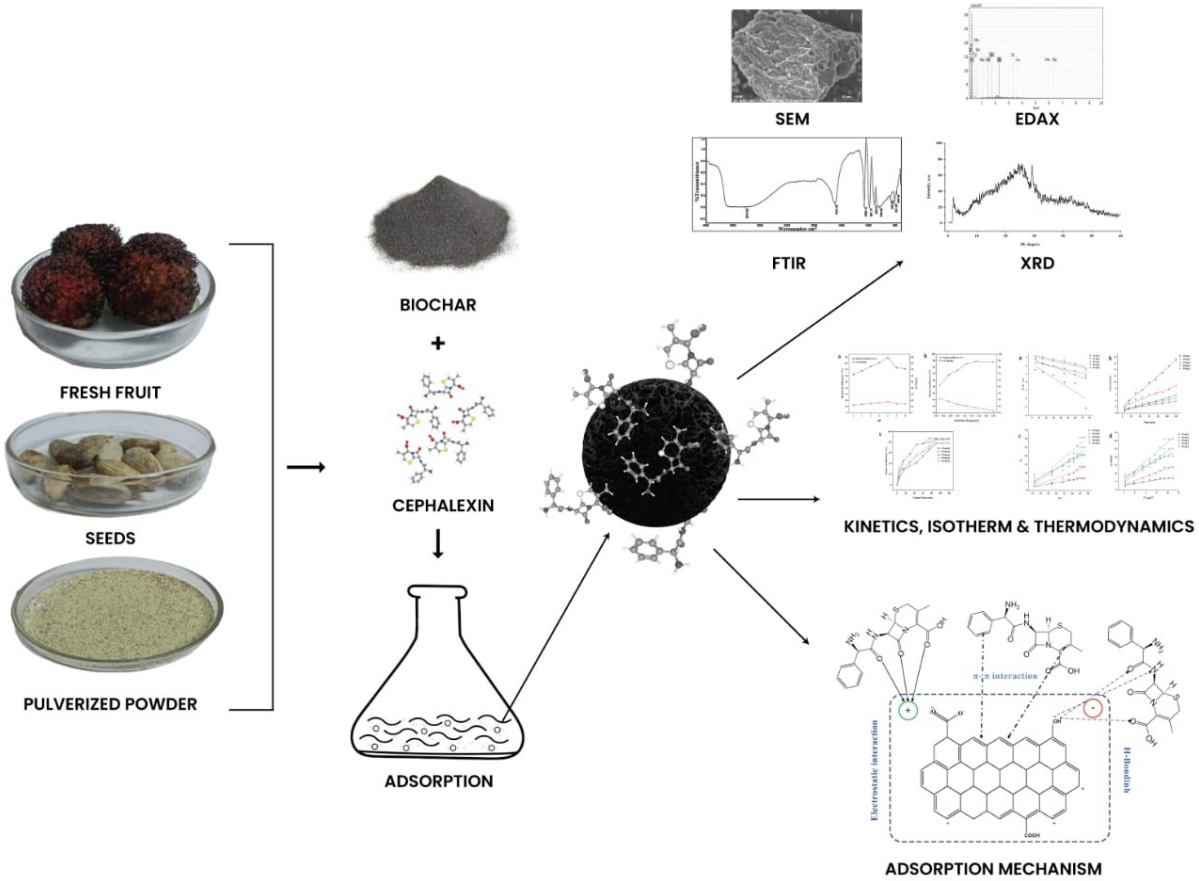

ABSTRACT

The improper disposal of drugs into bodies of water has become a severe environmental and health issue. Biochar synthesized from different agro residues could be a potential material for the adsorption of pollutants in aqueous environments. *Nephelium lappaceum* seeds were pyrolyzed at 600 °C in a pyrolysis reactor incorporating a slow pyrolysis process for carbonization. Fourier-Transform Infrared (FTIR), Scanning Electron Microscope (SEM), and X-ray diffraction (XRD) were used to characterize the biochar before and after adsorption of the pharmaceutical pollutant cephalexin. The effects of several factors, including initial cephalexin concentration, time of contact, dosage of adsorbent, and pH, were considered for the sorption. The findings showed that the Freundlich model offered the greatest fit for adsorption. The better-fitted kinetic model was the pseudo-second-order kinetic. Based on Langmuir isotherm model, the maximum adsorption capacity of cephalexin was obtained as 63.69 mg/g. The adsorption process involves hydrogen bonding, surface complexation, electrostatic and π–π EDA interactions. The current study offers a feasible and optimistic method for using agricultural waste and an alternative adsorbent substance for recovering highly concentrated cephalexin from water-based solutions.

Keywords: Drug disposal, Antibiotics, Biomass waste, Isotherms, Kinetics

1. INTRODUCTION

One of the most significant moments in medical history was the discovery of antibiotics, and according to statistics, more than 200,235 metric tons of antimicrobial agents will be required to eradicate growth and prevent bacterial diseases (Xu *et al.* 2022). Cephalexin, often known as CPX and having the technical name 7-(D-a-Amino-a-phenylacetamido)-3-methyl-3-cephem-4-carboxylic acid monohydrate ($C_{16}H_{17}O_4\ N_3SH_2O$) with a molecular mass of 365.40 g/mol, is an antibiotic of the first generation called cephalosporin, with an annual consumption of 3,000 tons. CPX is one of the world's most widely-used antibiotics,

according to reports. It belongs to the class of antibiotics known as beta-lactams and is discharged into the environment through sewage, hospital wastewater, pharmaceutical companies, animals, and agriculture. Environmental exposure to β-lactam antibiotic compounds occurs because of their use as components or intermediates for internal use (Wang *et al.* 2021). The continuous entry of CPX into the environment and water supplies will lead to environmental difficulties and issues for humans. To maintain water quality and safeguard public health, it is crucial to remove antibiotics, including CPX, from contaminated aqueous media (Arab *et al.* 2022). There are several innovative methods for eliminating antibiotics, including photocatalysis, fenton oxidation, ozonation, wet oxidation, membrane technology, adsorption, hybrid technology, aerobic and anaerobic treatment, and electrochemical oxidation. Among various methods for antibiotic removal, adsorption is highly effective because of its versatility, high selectivity, and ease of implementation across diverse water sources, offering several advantages in the process. Adsorption methods are employed to remove organic, inorganic, heavy metals, and microplastics (Phoon *et al.* 2020, Varma *et al*. 2024).

When organic raw materials are pyrolyzed in a low-oxygen environment to form biochar, a carbon-rich substance, as indicated above, the feedstock can come from a variety of sources (Wang *et al.* 2019). Because of its porous nature, substantial surface area, functional group incorporation, elevated capacity for cation exchange (CEC), and efficient removal of contaminants, biochar, a sustainable resource, serves as a proficient adsorbent (Karthik *et al.* 2023). Through pore filling, surface sorption, electrostatic interaction, π orbital interactions, electrostatic interaction, and ion exchange mechanisms, biochar eliminates contaminants (Al-Gheethi *et al.* 2021). Biochar can also be represented as BC, which can be made from agricultural and other natural waste components such as fruit seed waste. Many studies have documented biochar synthesis from seed waste biomass such as watermelon seeds, mango

seeds, jackfruit seed waste, *Prosopis juliflora* seed waste, and *Schizizium commune* seed to obtain low-cost substances that can be used for the elimination of several environmental contaminants, mainly heavy metals, dyes, and antibiotics (Periyasamy *et al.* 2022, Velusamy *et al.* 2021, Khadem *et al.* 2023, Diaz-Uribe *et al.* 2022, Kandasamy *et al.* 2022). As an alternative adsorbant, *Nephelium lappaceum* fruit seeds were used to generate biochar to eliminate cephalexin.

The tropical fruit *Nephelium lappaceum*, also referred to as rambutan, is indigenous to Southeast Asia and some portions of India under appropriate conditions, particularly in the southern sections. The fruit, characterized by a hairy, red or yellow outer skin and translucent, juicy flesh with seeds within the fleshy aril, provides a promising feedstock for biochar production because of the seeds' high cellulose content and unique chemical composition. The process involves subjecting the seeds to pyrolysis and thermochemical decomposition without oxygen, resulting in the transformation of the biomass into a stable, carbonaceous material with a porous structure. The cation exchange capacity, high surface area, and functional groups of BC derived from rambutan seeds are all potentially advantageous features. Despite being consumed globally for its health benefits, the unpalatable nature of rambutan seeds has led to their disposal. Converting these discarded seeds into biochar offers a potential solution for effective by-product use (Batool *et al.* 2022, Naveen and Muthumari 2024). To overcome some of the shortcomings of conventional adsorbents with low kinetics and poor adsorption capacity, *Nephelium lappaceum* seed biochar was employed as an adsorbent for successful antibiotic removal.

In this study, biochar was prepared using *Nephelium lappaceum* seeds under pyrolysis. Biochar was used to adsorb cephalexin. FTIR, SEM with EDAX, and XRD were used to characterize the synthetic biochar. The impacts of various operating parameters, such as pH, temperature, contact time, and cephalexin concentration, were also investigated. Furthermore,

the adsorption process was determined by analyzing the characteristics of the biochar before and after cephalexin adsorption, as well as examining the adsorption kinetics, isotherms, and thermodynamics.

2. EXPERIMENTAL

2.1 Collection of Biomass and Biochar Preparation

Nephelium lappaceum seeds were collected from a nearby village located near Tenkasi, Tamil Nadu, India. After thorough cleaning with tap water and deionized water, it was left to dry for 3 days under sunlight. To remove the last traces of moisture the seeds were kept in an oven at 50°C for 2 days over night. After drying, it was crushed with a mortar and pestle and used to make biochar (BC). *Nephelium lappaceum* seeds that had been processed were pyrolyzed in a furnace carbonized at 600°C for one hour at a heating rate of 3°C/min with slow pyrolysis. The oxygen-free environment in the pyrolyzer was achieved by purging inert gases such as nitrogen before and during pyrolysis. The produced BC was removed from the furnace and then cooled to room temperature in desiccator. For later use, *Nephelium lappaceum* seeds BC were kept in an airtight container (Chakraborty *et al.* 2018, Venkateswaran *et al*. 2023).

2.2 Preparation of Cephalexin Solution

Commercially available cephalexin -250 mg tablets were purchased in their impure form. The tablets were available in powdered form it was dissolved in the distilled water after removing their outer covering. The optimal wavelength for cephalexin was determined using UV/visible spectrometry. A 100 ppm stock solution of cephalexin was prepared in a 250 mL volumetric flask. From this stock solution, standard solutions with cephalexin concentrations of 2, 4, 6, 8, 10, 12, and 14 ppm were prepared. The optimized wavelength obtained was 251 nm (Velusamy *et al.* 2021).

2.3 Point of Zero Charge

The pH Point of Zero charge (pzc) was ascertained by adding salt with BC. Twenty milliliters of 0.1M $NaNO_3$ solutions were prepared by varying the pH from 3 to 12 at every 1 pH interval, which is represented as the initial pH (pH_i).After adding 0.20 g of biochar, the aforementioned solutions were stirred for a whole day.The solution's final pH (pHf) was measured after 24 hours. Plotting the graph of (pH_i-pH_f) versus (pH_i) showed the pzc value (Adam *et al.* 2016).

2.4 Characterization of Biochar

The morphology of the surface of the sample was analyzed by SEM-EDAX (Supra 55-Carl Zeiss, Germany). In order to investigate the structure and crystalline character of biochar before and after adsorption, XRD test was conducted at a voltage of 9 kW and radiation of ƛ = 1. 54 Å (Rikagu Japan). Functional groups present in the BC were determined using FTIR (Shimadzu 8400s) before and after adsorption within a wavenumber region of 0 to 4000 cm^{-1} (Li *et al.* 2018).

2.5 Batch Adsorption Study

Batch adsorption studies were evaluated using the synthesized BC to remove cephalexin (CPX). To determine the effects of agitation time (0 to 120 mins), initial cephalexin concentration (10 to 50 mg/L), BC dosage (0.05 to 0.2 g/L), pH (2-8), and temperature (303.15 to 333.15K), the removal of CPX was tested under various experimental conditions. After optimizing the parameters, the adsorption isotherms were determined. 100 mL of CPX solution was taken in 250 mL conical flask containing BC sample was kept in an orbital shaker (Neolab Incubator Shaker) with an agitating speed of 150 rpm. A PTFE filter with a mesh size of 0.45µm was used to filter the sample, and to quantify concentration, a UV-visible spectrophotometer at a wavelength of 251nm was utilized (Dai *et al.* 2020). In this study, the adsorbed CPX concentration $q_{(t)}$ was determined using the following equation:

$$q_{(t)} = \frac{V\,(C_o - C_t)}{W} \qquad (1)$$

where V - denotes the sample volume (L), W - represents the adsorbent mass (g), and C_0 is the initial concentration of CPX in solution (mg/L) and C_t - represents the concentration of cephalexin at time t (mg/L).

2.6 Adsorption Isotherm

The adsorption isotherms of CPX, a BC dose of 1.25g/L and pH 6 were maintained throughout the experiment. After adding BC, the temperature 30° C and contact time was 90 min. Then, the adsorption isotherms of cephalexin by *Nephelium lappaceum* BC were performed through isotherm models such as Langmuir (Equation2), Temkin (Equation3), and Freundlich (Equation4).

$$\frac{C_e}{q_e} = \frac{1}{q_m} K_L + \frac{C_e}{q_m} \quad (2)$$

$$q_e = \frac{RT}{b_T} lnK_T + \frac{RT}{b_T} lnC_e \quad (3)$$

$$lnq_e = lnK_f + \frac{1}{n} C_e \quad (4)$$

where, K_L illustrates the Langmuir constant with respect to adsorption energy and q_m represents the maximum sorption capacity (mg/g), K_f indicates the Freundlich sorption capacity (mg/g), and the symbol n denotes the Freundlich constant, a measure of the attraction between the adsorbent and the adsorbate that is correlated to surface heterogeneity, the heat of adsorption is related to the Temkin constant (b_T), the maximal binding energy (L/mg) is related to the equilibrium binding constant (K_T), the ideal gas constant (8.314 J/mol/K) is related to R, and the absolute temperature is related to T (K) (Karthik *et al.* 2020).

3. RESULTS AND DISCUSSION

3.1 Characterization Studies

3.1.1. FTIR analysis

The FTIR spectra of the produced biochar and the one with and without antibiotics showed the functional groups on the surface of the biochar (Figure 1). It is imperative to identify functional groups, which include organic, inorganic, and polymeric functional groups when synthesizing biochar to understand the adsorption properties of the produced biochar. It should be noted that the functional groups in the BC atoms may not be an exact match due to molecular interactions that can affect the BC atoms, as seen from the FTIR spectra of the samples. The FTIR spectra of the *Nephelium lappaceum* seed-derived biochar and the corresponding FTIR spectra after CPX adsorption were obtained over the range of 400–4000 cm^{-1}. The results depict that there are large bands in the region 3400-3300 cm^{-1}, which is the characteristic of O-H stretch owing to hydrogen bonding. This peak shifts from a broad peak at around 3400 cm^{-1} after adsorption to a narrower range between 3300 cm^{-1} and 3200 cm^{-1}. The C-H group is seen at 2920 cm^{-1} only in BC which suggests that hydrogen is quite significantly displaced during the adsorption of CPX. The peaks located at 1652 cm^{-1} and 1624 cm^{-1} are the carbonyl C=O group that is present before and after the samples' exposure to CPX. The small peaks at approximately 1515 cm^{-1} and 1547 cm^{-1} can be attributed to C=C stretching. Also, the shift of the peak at around 1600 cm^{-1} associated with the C=C bond of phenol and the new peak at 1080 cm^{-1} for C-O in the phenol bond after the adsorption of CPX. The peaks involved in the metal hydroxyl stretch that falls in the 1000-400 cm^{-1} region of both spectra is assigned to the metal adsorption region (Velusamy *et al.* 2021, Dai *et al.* 2020). By analyzing the relative intensities and positions of the spectra peaks, it is shown that there is a good interaction between CPX and the functional groups, which are parts of the biochar structure. A comparative analysis of the changes in the peak intensities associated with OH and C-H functional groups demonstrate enhanced interaction between the molecules and hydrogen abstraction in the course of adsorption (Karthik *et al.* 2020, Martins *et al.* 2015, Miao *et al.* 2016). The results provided by the spectra, showing the carbonyl and

phenol groups on the surface of the samples, as well as their absence after the adsorption process prove their importance in the process. The metal hydroxyl stretch being present all the time point out that the areas where the metal is adsorbed are in the process of being formed. The results of this study also point towards functional groups as significant for the adsorption of CPX by *Nephelium lappaceum* biochar.

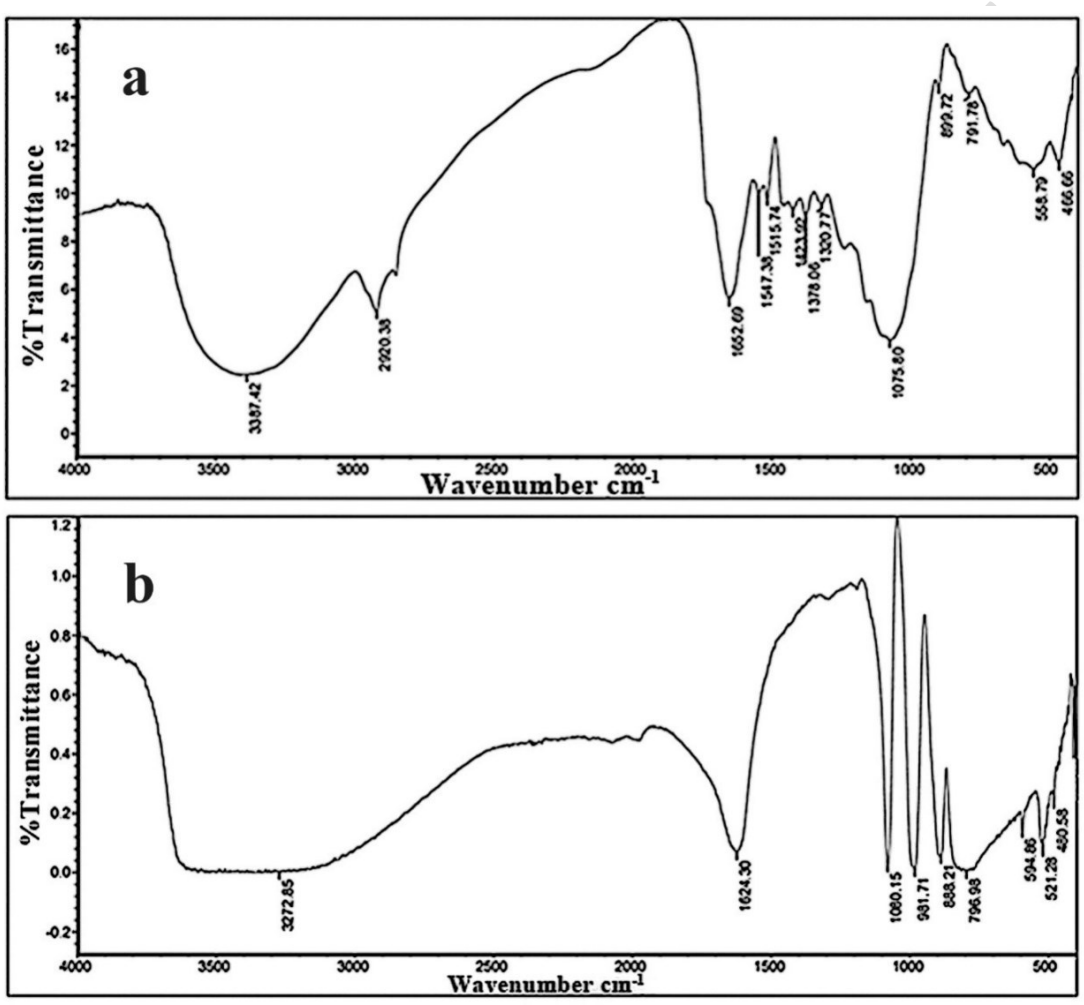

Figure 1. FTIR graph for before adsorption (a) and after adsorption (b) of cephalexin using biochar.

3.1.2. XRD Analysis

XRD analysis was made before and after the adsorption of CPX by biochar (BC), as illustrated in Figure 2. The untreated CPX in BC was characterized by scattering angle found at 2θ = 24.42, 30.61, and 40.09, which indicates that BC is an anhydrous crystal structure.

Similarly, the XRD pattern of CPX-treated BC displayed a broad peak at 2θ = 19.92, 24.89, and 43.89, which was reported to be crystalline in nature (Mondal *et al.* 2018, Topal *et al.* 2020). The BC showed an increased d value (interlayer space) of 4.453º due to the interactions of the organic molecules in the BC, which were also confirmed by the FTIR results. When CPX was treated with BC, the d value was decreased to 3.641º. The surface-active sites of BC bind to the CPX functional group, resulting in a grafting reaction. A similar behavior was reported in (Ashiq *et al.* 2019).

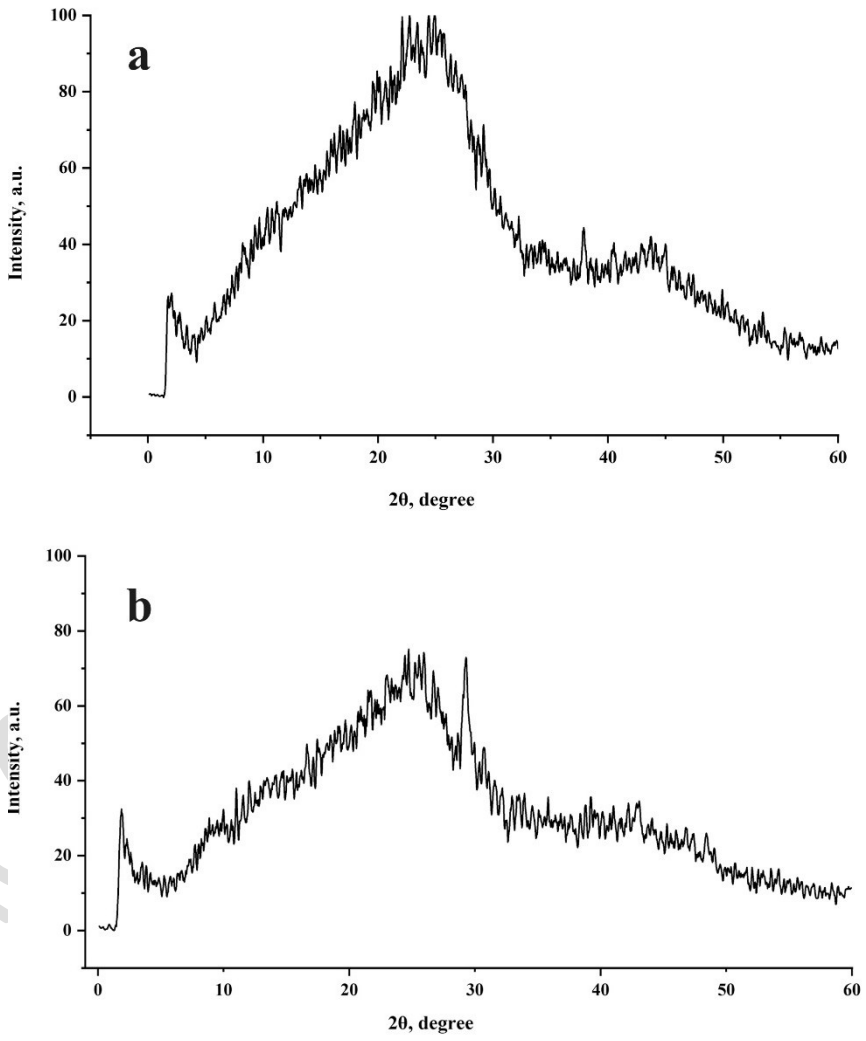

Figure 2. XRD analysis of before adsorption (a) and after adsorption (b) for cephalexin using biochar.

3.1.3. SEM –EDAX analysis

The SEM image before and after the adsorption of CPX by *Nephelium lappaceum* BC is shown in Figure 3a. The sample was examined using SEM to determine whether *Nephelium lappaceum* BC took up CPX. It is also employed to examine BC pore size, shape, and structure that favors cephalexin adsorption. Figure 3a shows that *Nephelium lappaceum* BC, before adsorption,was a non-uniform pore over the surface area. Incontrast, the SEM image in Figure3b represents the clump-like structure of cephalexin 250mg, effectively adhering to *Nephelium lappaceum* BC's pores. CPX is primarily adsorbed by *Nephelium lappaceum* BC because of its large pores, as shown in Figure 3b. The results obtained were compared with the SEM image of the reported soap nut seed biochar (Velusamy *et al.* 2021). The elemental composition before and after the adsorption of CPX by *Nephelium lappaceum* BC was analyzed using EDAX. The primary organic components of CPX are carbon and oxygen. The addition of CPX is implied by variations in the adsorbent's elemental contents, particularly carbon and oxygen weight percentages, before and after adsorption, as shown in Table 1and Figures 3c and 3d. It was shown that the absence of sulphur and maganese in BC before adsorption. The peak of sulphur and maganese was observed in the EDAX spectra of CPX adsorption by *Nephelium lappaceum* BC, which confirmed the adsorption process. Oxygen, carbon, sodium, calcium, potassium and iron atoms are presented before and after adsorption. In addition, it was also found that the element C decreased by about 2% by weight, Na and Ca increased by 55% and 54% by weight. O was found to be increased by 2.5 weight % while other elements did not change much (Chakraborty *et al.* 2018, Topal *et al.* 2020).

Table1. Elemental composition of BC before and after CPX adsorption.

	Map sum spectrum	
	Before adsorption	After adsorption
Components	Mass %	Mass %

C	88.18	86.19
O	10.67	10.94
Na	0.41	0.92
Ca	0.31	0.68
Al	0.04	0.57
K	0.24	0.45
S	-	0.10
Fe	0.11	0.07
Si	0.03	0.05
Mn	-	0.04

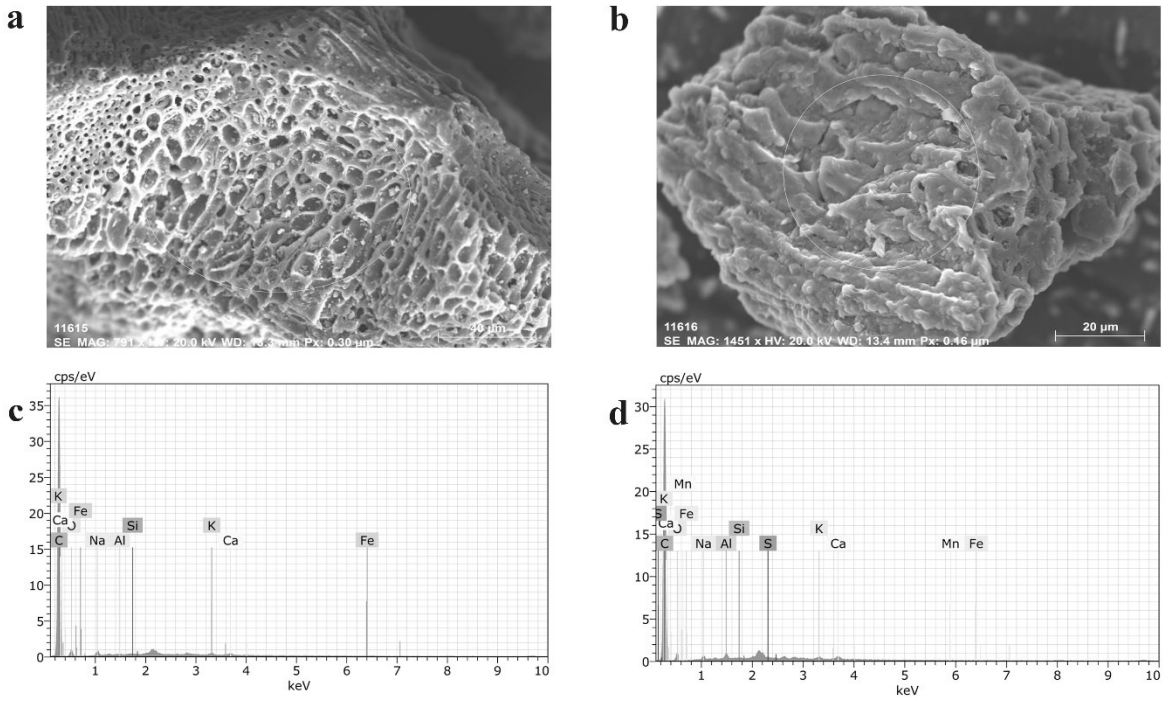

Figure 3. SEM image (a) before adsorption, (b) after adsorption of CPX, Elemental analysis (c) before and (d) after adsorption of CPX

3.2. Point of Zero Charge

The quality of the relationship between pH and antibiotic adsorption can be assessed using the Point of Zero Charge (pHpzc). Zero charge theory states that because there are less OH- ions on the surface of biochar with pH values below pzc, the surface is positively charged, and when pH values exceed pzc, the surface is negatively charged because there are more OH-ions. The surface charge of the biochar can be determined by performing pHpzc and it was reported as 8.5 which was shown in figure 4. Generally, the antibiotic Cephalexin (CPX) is in the zwitterionic form, which implies it has both positive and negative charges. In this regard, if pH less than pHpzc, the surface of biochar carries positive charge which may interact with negative charge of the antibiotic due to electrostatic interactions. Furthermore, increase in pH values higher than pHpzc the surface of biochar will became negatively charge does not encourage the electrostatic interactions due to higher concentration of OH^- ions (Dehghan *et al.* 2019). Similar results were reported the electrostatic interactions of CPX and *Anthriscus sylvestris* derived activated biochar by performing the pHpzc (Shirani *et al.* 2020).

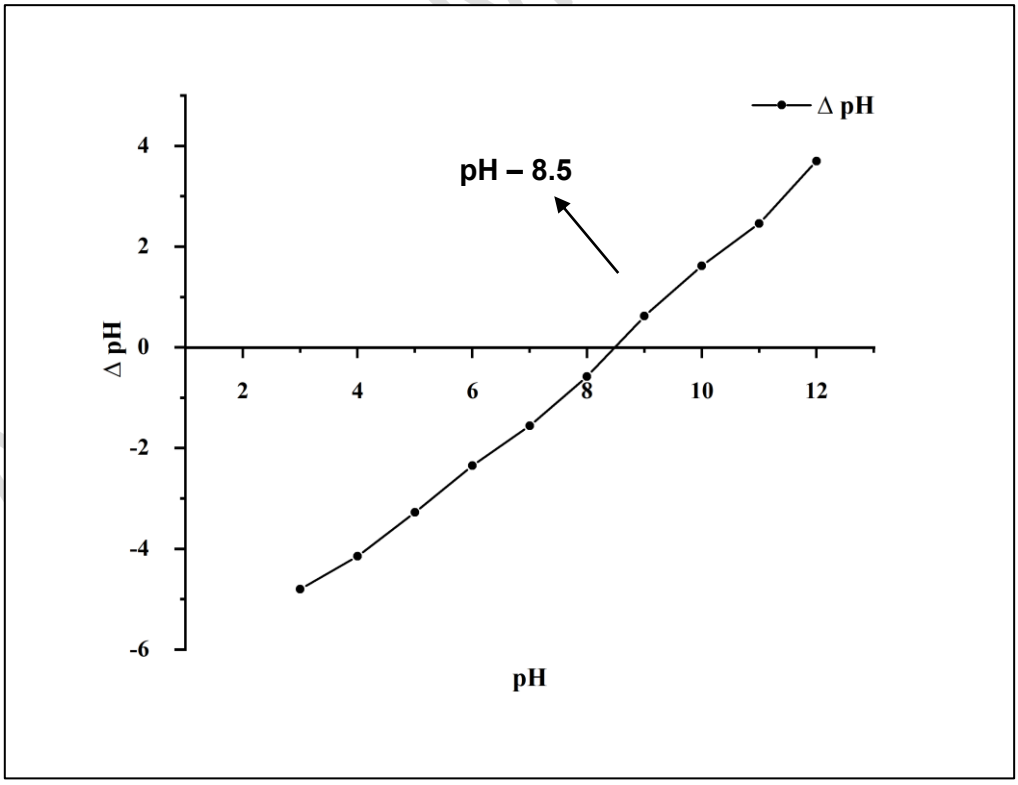

Figure 4. Determination of pH pzc for *Nephelium lappaceum* seeds BC.

3.3. Parameter Optimization

3.3.1. Influence of pH

The mechanism by which the adsorbate and adsorbent interact is significantly influenced by pH. Figure 5a illustrates the removal of CPX with respect to pH and adsorption capacity. To investigate the elimination of CPX, the pH was altered from 2 to 8. CPX can be found in the form of zwitterion which implies the presence of positive and negative charges encourages the adsorption through electrostatic interactions. From the result of pHpzc, as the pH increases from 2-6, the surface charge of biochar interacts with the negatively charged antibiotic by electrostatic interactions which results in increased removal efficiency causes an increased adsorption efficiency. The maximum removal efficiency was reported in pH 6 with 89% removal efficiency r_f and adsorption capacity q_e17.80 respectively. Further rise in pH, removal efficiency reduced. This may be due to higher concentration of OH^- ions which results in lower adsorption efficiency. Similar findings were stated from the study of cephalexin removal by green synthesis of nanocomposites using pomegranate peel which relates the impact of pH and the adsorption process are due to the electrostatic interactions (Rashtbari *et al.* 2020, Priyadharsini *et al*. 2023).

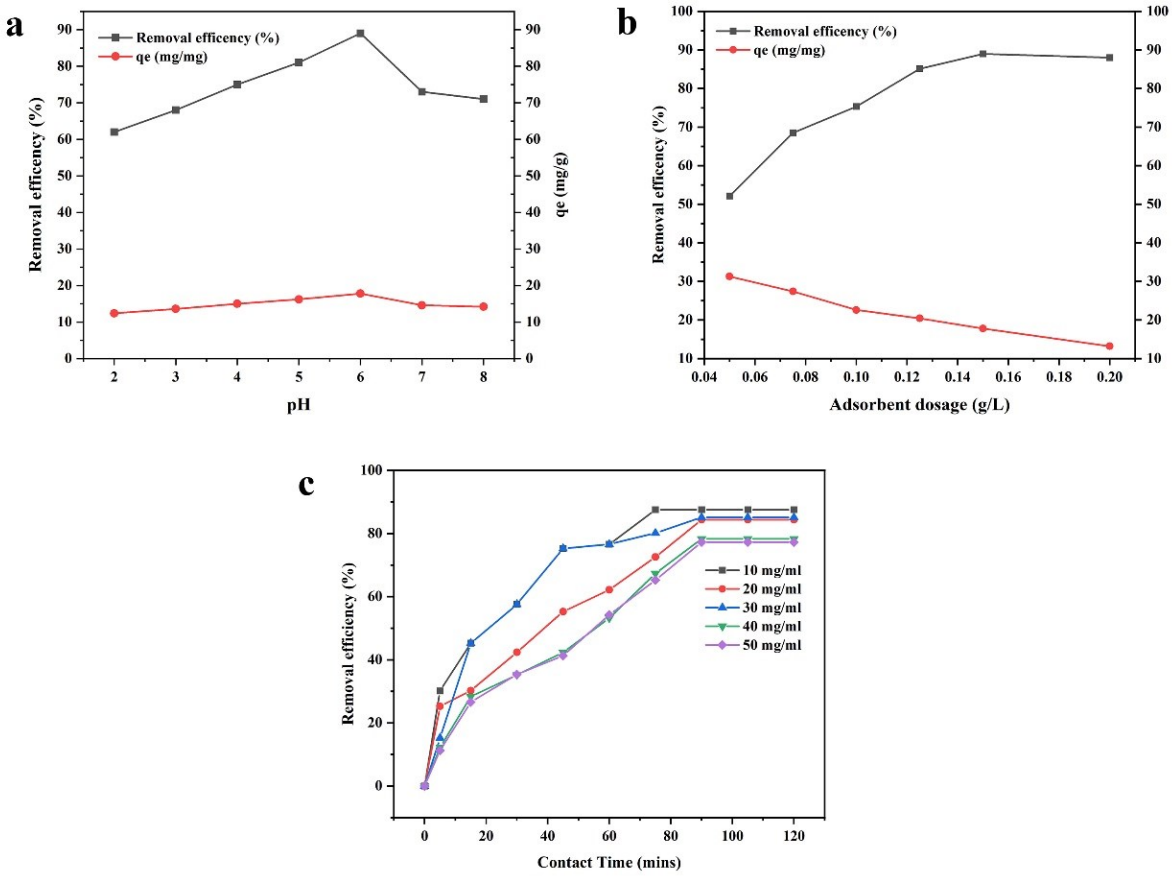

Figure 5. Parameter optimization a) Influence of pH b) Influence of biochar dose with respect to adsorption capacity and c) Influence of Contact time and Initial CPX Concentration with respect to removal efficiency

3.3.2. Influence of biochar dose

The influence of adsorbent dose on removal efficiency and adsorption capacity was shown in figure 5b. From the figure, it was noted that as adsorbent dosage increases with increase in removal efficiency from 52.79% to 87.23%respectively. This increasing trend of removal efficiency is due to the existence of more adsorption site as well as higher surface area present in the biochar. Conversely, when the adsorbent dose was increased from 0.5 to 2 g/L, the adsorption capacity declined. The adsorption capacity range was reduced from 31.6 to 17.37 mg/g. At higher dose of biochar accumulation reduces the availability of active surface sites results in lower adsorption capacity. The optimal adsorbent dose was determined to be

1.25g/L, and when the adsorbent dosage increased, the removal efficiency and adsorption capacity remained constant. Similar trend was already reported in Miao *et al.* 2016.

3.3.3. *Effect of Contact time and Initial CPX Concentration*

In order to examine the impact of contact time and initial CPX concentration, the experiments were carried out by adding 1.25g/L of the biochar into flasks containing CPX initial concentration varying from 10 to 50 mg/L. Figure 5c showed the effect of contact time ranged from 10 to 120 mins. Initially the CPX adsorption was fast in the first 60 mins and decline slowly then finally reaches equilibrium. The equilibrium was reached at 90 mins. Further increase in contact time does not result in significant amount of rise in removal efficiency. Initially the adsorption was fast because there is the availability of more adsorption sites present in the adsorbent at the initial stage of adsorption (Miao *et al.* 2016).Similar results were recorded by Rashtbari *et al.* 2020.

3.4. Adsorption Kinetics

The effect of contact time (0-120min) was investigated for CPX adsorption onto BC with varying initial CPX concentration (10 to 50 mg/L), adsorbate dosage -1.25g/L and pH -6. From figure 8 it was clear that initially increases rapidly in the adsorption rate and reaches equilibrium at 90 mins this is due to the higher concentration of CPX in solution and high availability of adsorption site in the BC surface. After it reaches equilibrium the adsorption rate decreased due to the lesser concentration of CPX as well as low availability of vacant sites (Rashtbari *et al.* 2020).The rate of CPX adsorption on BC was analyzed through kinetic studies: Pseudo-first order kinetics, Pseudo-second order kinetics, Elovich kinetics, Intraparticle diffusion kinetic model.

3.4.1. *Pseudo-first order kinetics*

Pseudo –first order kinetics occurs when the concentration of one reactive molecule is kept constant or in excess. The equations used to determine the Pseudo-first order kinetics studies are mentioned in eq (6)

$$\ln(q_{e-}q_t) = lnq_e - K_1 t \quad (6)$$

The equilibrium rate constants for pseudo-first (PFO) kinetics is K_1 (min^{-1}). Figure 6a represents the linear plot ln (q_e-q_t) versus t at various concentration of CPX antibiotics indicating the intercept equal to K_1 and ln (q_e) as slope. The amounts of adsorbed CPX at equilibrium and time 't' are represented as q_e (mg/g) and q_t (mg/g). Table 2 represents the linear regression coefficient values and constants for pseudo first order kinetics. R^2 values ranges from 0.802 – 0.969 which infers relatively low R^2 values compared to other kinetics and the K_1 values for various concentrations ranges from (0.019- 0.065). The adsorption kinetics data shows a deviation from straight line and implies that pseudo first order kinetics does not fit well for CPX adsorption with the biochar. The obtained findings were same with the Cu^{2+} adsorption with *Manikara zapota* sees biochar (Karthik *et al.* 2023).

3.4.2. Pseudo-second order kinetics

The pseudo-second order model describes the chemical adsorption process which influence electrostatic forces and it is considered as the rate limiting step in adsorption process.The equations used to determine the Pseudo-second order kinetics studies are mentioned in eq (7)

$$\frac{1}{q_t} = \frac{1}{K_2 q_e^2} + \left(\frac{1}{q_e}\right) t \quad (7)$$

Equation (7) obeys Pseudo second order kinetics where K_2 is the rate constant. Figure 6b plotted between (t/q_t) versus t at different concentration. Table 2 and figure 6b represents pseudo second order kinetics shows higher R^2 value indicates better fit and the rate of adsorption was controlled by chemisorption. The findings presented here are supported by a chemisorption process that is compatible with the kinetic adsorption behavior reported in reference (Ma *et al.* 2020).

3.4.3. Elovich Kinetics

Elovich model suggests the surface is heterogeneous and supports the second order kinetics (Zhang *et al.* 2021). The equations used to determine the Elovich Kinetics studies are mentioned in eq (8)

$$q_t = \frac{1}{\beta} ln(\alpha\beta) + \frac{1}{\beta} \ln t \quad (8)$$

The adsorption capacity was calculated using equation (8), where α represents the initial adsorption rate and β denotes the desorption constant. From table 2 and figure 6c the values of R^2 ranges from (0.839-0.966) and the initial adsorption rate value was increased from 1.27-3.07 as the concentration increases from 10mg/L to 30 mg/L, indicates the second best fit and it also confirms the process is chemisorption. Similar responses were reported in cephalosporin antibiotic adsorption using soap nut biochar (Velusamy *et al.* 2021).

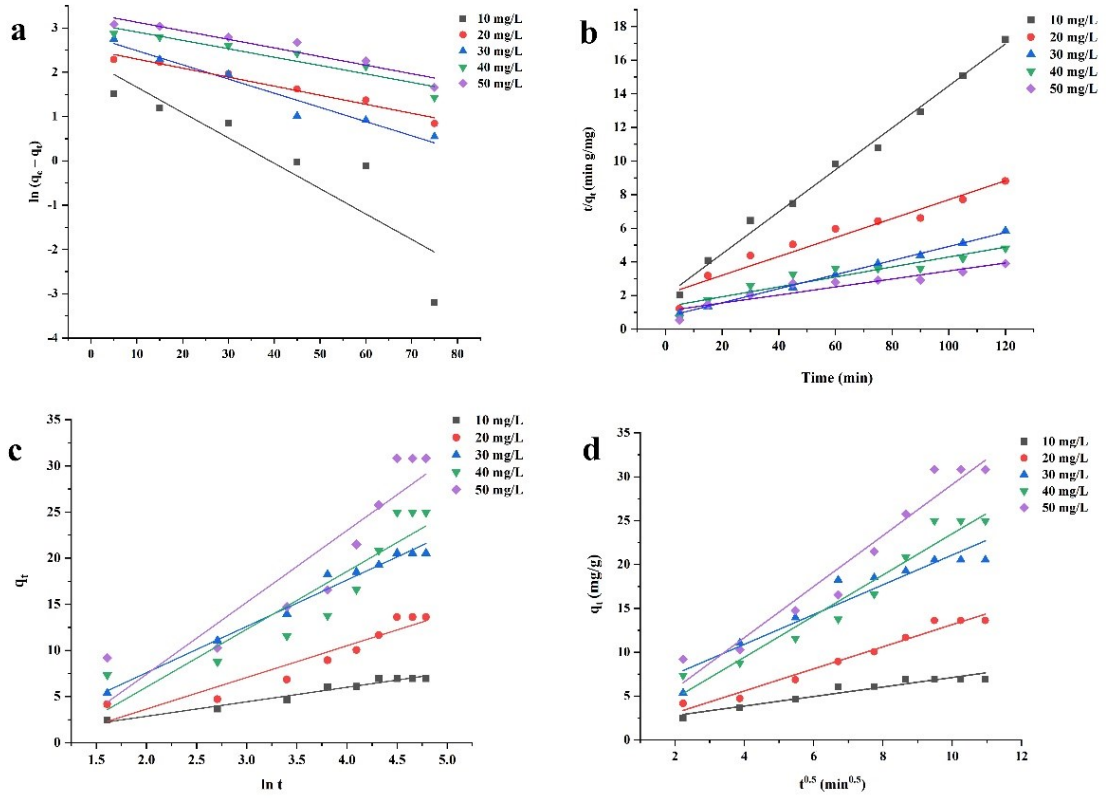

Figure 6. (a) Pseudo first order(b) Pseudo second order(c) Elovichand (d) Intraparticle diffusion at varying contact time (min), pH 6.0, 1.25 g/L adsorbent dosage, Initial concentration 10 – 50 mg/L.

3.4.4. Intraparticle Diffusion

Intraparticle diffusion is considered as rate limiting step in the adsorption process. The adsorption capacity was calculated using the following eq (9)

$$q_t = K_p t^{0.5} + C \quad (9)$$

The linear plot was plotted between q_t versus $t^{0.5}$ and it is represented in the figure 6d where C is the constant related to thickness of the boundary layer and K_p is the rate constant for intraparticle diffusion. C and Kp values were computed from the graph using the intercept and slope as parameters. If the C value increases, then the boundary layer effect will be more whereas from the table 2 it was clear the intercept value is small indicating lower boundary layer effect.

If adsorption is regulated by intra particle diffusion, the plot of qt vs $t^{0.5}$ should pass through origin. From the plot it was concluded that the adsorption process is not dominated by intra particle diffusion. Elimination of tetracycline by hazelnut shell biochar yielded similar results (Fan *et al.* 2016).

Table 2. Kinetic parameter of PFO, PSO, Elovich and Intraparticle diffusion for the BC.

Initial Concentration (mg/L)	PFO kinetics			PSO kinetics			Elovich kinetics			Intraparticle diffusion		
	q_e mg/g	k_1 min^{-1}	R^2	$q_e$mg/g	k_2 min^{-1}	R^2	α mg/g min	β g/mg	R^2	k_p mg/g $min^{0.5}$	C mg/g	R^2

10	9.35	0.057	0.801	8.00	0.007	0.99	1.27	0.65	0.966	0.54	1.69	0.927
20	12.20	0.020	0.969	17.76	0.002	0.94	1.34	0.29	0.894	1.24	2.54	0.970
30	17.11	0.033	0.951	23.92	0.0023	0.99	3.07	0.19	0.979	1.69	4.10	0.901
40	22.14	0.065	0.805	33.78	0.0006	0.875	2.21	0.15	0.839	2.35	0.03	0.947
50	27.72	0.019	0.914	41.84	0.0005	0.878	2.73	0.12	0.842	2.92	0.02	0.95

3.5 Adsorption Thermodynamics

The thermodynamic studies were conducted for CPX at varying temperatures (303.15, 313.15, 323.15 and 333.15 K) were analyzed by eq (10). The linear plot was plotted ln K_L against 1/T (Figure 7) and the thermodynamic parameters such as ΔS° and ΔH° were determined from the slope and intercept values of the graph and it was summarized in table 3.

Table 3. Thermodynamic factors for CPX adsorption under various temperatures.

Temp (K)	ΔG^o(J/mol)	$-\Delta H^o$(J/mol)	$-\Delta S^o$ = (J/mol)
303.15	-4247.551	9.996	19.091
313.15	-3951.587		
323.15	-3839.413		
333.15	-3653.311		

$$\Delta G^o = -RT\ln K_L \quad (10)$$

The values of Gibbs free energy changes from -4247.551, -3951.587,-3839.413 and -3653.311 J/mol for CFX adsorption on BC at 303.15, 313.15, 323.15 and 333.15 K. The G values were negative, revealing that the CPX adsorption mechanism was spontaneous in nature. Increase in temperature results in increase in Gibbs free energy value implies the

possibility of adsorption at higher temperature. The ΔH value for CPX adsorption was found to be -9.996 J/mole. The result confirmed the nature of adsorption to be exothermic. Similarly, ΔS value found to be -19.091J/mol which denotes the decrease in the degree of randomness at absorbate and adsorbent interface in the process of adsorption (Ahmed et al. 2012). Similar results were reported on cephalexin removal using *Albizia lebbeck* seeds pods by microwave induced KOH and K_2CO_3 activations.

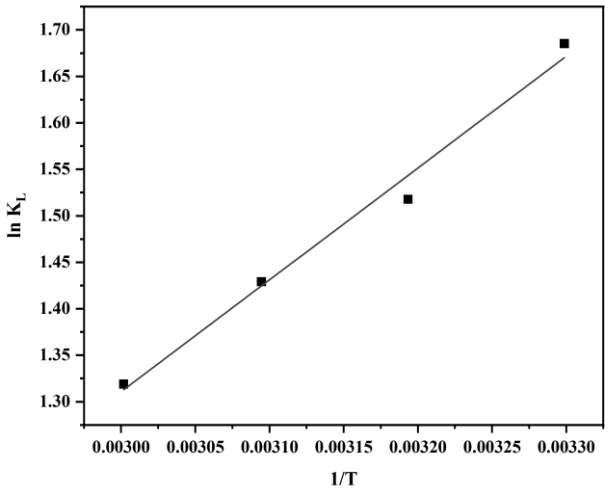

Figure 7. Thermodynamics graph between 1/T versus ln K_L.

3.6. Adsorption Isotherm Models

The technique by which CPX adsorbs on BC was investigated using adsorption isotherms. Dynamic phenomena of the adsorbate equilibrium distribution occur between an aqueous solution and an adsorbent. The isotherm models of Freundlich, Langmuir and Temkin described the process. To identify the better fit the parameters obtained from linear regression should be close to unity.

3.6.1 Freundlich Isotherm

The non-equal binding sites are explained by the Freundlich model, which illustrates a multiple-layer physical adsorption process on a heterogeneous surface. The linear graph was plotted between $\ln q_e$ versus $\ln C_e$. From the graph 8b K_f, R^2 and n values are calculated and it

was displayed in the table 4. From the table R^2 value was found to be 0.993. The adsorption of CPX by using *Nephelium lappaceum seeds* BC is well fitted with Freundlich isotherm. The parameter n is also identified as the heterogeneity factorto assess whether the adsorption process is physical (n > 1), chemical (n < 1), or linear (n = 1). The n value demonstrates that the process is physical and is found to be 1.35. The ratio 1/n provides information on the surface heterogeneity. Therefore, the closer1/n ratio approaches zero, the more heterogeneous the surface material is in nature. The obtained 1/n score 0.7396 indicates that the BC exhibits substantial heterogeneity (Tang et al. 2018, Pezoti et al. 2014).Comparable outcomes were noted when using coconut fiber biochar to remove Co (II) (Karthik *et al.* 2023).

3.6.2 Langmuir Isotherm

The theoretical maximum capacity for the adsorption of biochar, where there is no interaction among adsorbates and when an adsorbate is adsorbed onto an adsorbent's homogeneous surface, is identified using the Langmuir model, a single layer chemical absorption model (Karthik *et al.* 2023). The linear graph was plotted against C_e/q_e versus C_e. From the graph 8a K_L and q_m values were calculated and tabulated in table 4.As indicated by the table, the determination coefficient (R^2) was discovered to be 0.9574. The separation factor, or R_L, is a dimensionless metric that is utilized to identify whether the adsorption process is irreversible, unreversible, or favorable. The equation used to calculate R_L is represented in Equation 11.The Langmuir model fit into the adsorption process depends on adsorption capacity value and the implications are R^2 and K_L values.

Table 4. Langmuir, Freundlich and Temkin isotherm parameters for the adsorption of CPX on BC.

Isotherm models	Factors	R^2
Langmuir	q_m= 63.694(mg g^{-1})	0.957
	K_L=0.075(mg^{-1})	

Freundlich	K_f=5.060 ((mg $\cdot g^{-1}$ $\cdot(1/mg)^{1/n}$)	0.993
	n= 1.352	
Temkin	b_T=11.601	0.979
	K_T=1.012(mg^{-1})	

413

414 $$R_{L=\frac{1}{K_{LC_O}}} \quad (11)$$

415 R_L indicates whether biosorption is irreversible when (R_L = 0), linear (R_L = 1), feasible (0 <
416 R_L<1), or uncertain (R_L> 1). The separation factor value (R_L=0.325) suggests that the
417 physical adsorption approach is preferable (Acelas *et al.* 2021).The Langmuir model fit into
418 the adsorption process depends on adsorption capacity value and the implications are R^2 and
419 K_L values. From the R^2 values it was concluded that it does not fit well with Langmuir
420 compared to Freundlich isotherm.

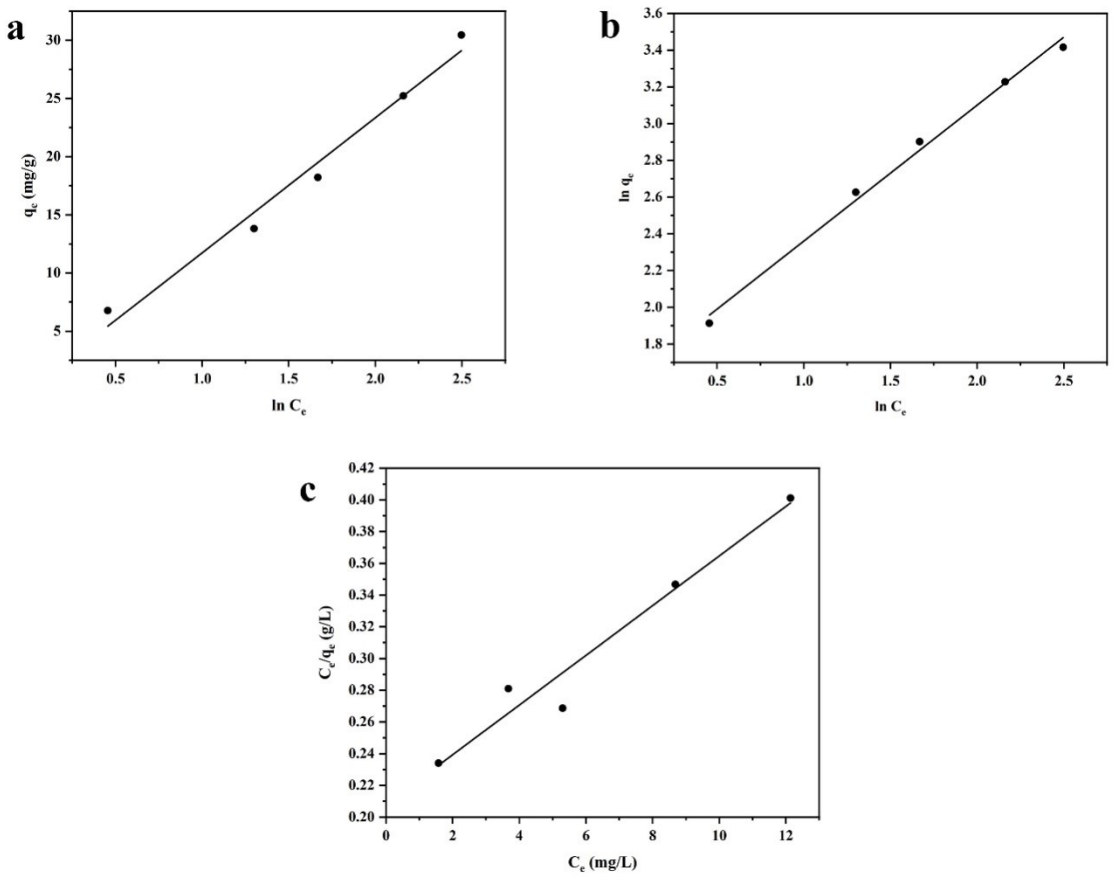

421 **Figure 8.** (a) Langmuir, (b) Freundlich and (c) Temkin isotherms at pH 6.0, 1.25g/L
422 adsorbent, initial concentration 10 –50 mg/L.

423

424

425 **3.6.3 Temkin Isotherm**

426 The Temkin model was used to demonstrate the chemisorption process. The dispersion of
427 interaction energies during the adsorption process and the linear decline in adsorption energy
428 with surface coverage is used to illustrate the chemical adsorption process (Liu *et al.* 2017,
429 Sun *et al.* 2016). The linear plot was plotted between ln C_e versus q_e. From the graph 8c R^2
430 value, b_T and K_T values were evaluated and it was tabulated in table 4. As indicated by the
431 table, the determination coefficient (R^2) was discovered to be 0.979. The adsorption is well

fitted with Temkin based on the regression coefficient. The adsorption energy variation is known as the Temkin constant, or b_T, and it determines whether an adsorption is exothermic when (b_T> 1) or endothermic (b_T<1). The CPX adsorption using BC that arises exothermically in various concentrations was examined according to the b_T value of 11.601. Comparable outcomes were noted when using coconut fiber biochar to remove Co (II) (Karthik *et al.* 2023).

3.7 Potential Adsorption Capacity of Adsorbents

Table 5 illustrated the cephalexin adsorption capacities of the organic adsorbents. These methods have two drawbacks: low reactiveness and a complicated preparatory process. Biochar has a distinct surface area and pore structure because of the existence of particular functional compounds like hydroxyl or carboxyl groups. The economic feasibility of employing BC in water treatment is also influenced by its chemical makeup and potential for regeneration and reuse. In contrast to these adsorbents, the overall carbon footprint of the BC production procedure may be calculated by considering the energy consumed during pyrolysis, the sustainability of the biomass supply, and the entire carbon footprint of the pyrolysis process. Because of its relatively easy production method and reasonably good adsorption capacity, *Nephelium lappaceum* seed BC could be an efficient adsorbent.

Table 5. Adsorption capacity of cephalexin using biochar

Adsorbent	Adsorption capacity mg/g	References
Oil palm fiber biochar	7.9	[Grisales-Cifuentes *et al.* 2021]

Natural zeolite	16.1	[Samarghandi *et al.* 2015]
Activated carbon	17.361	[Al-Khalisy *et al.* 2010]
Activated carbon from lotus	38.80	[Liu et al. 2011]
Alligator weed biochar	45.00	[Miao *et al.* 2016]
Activated carbon from pomegranate peel	48.78	[Rashtbari *et al.* 2020]
Palm oil fiber biochar	57.47	[Sun *et al.* 2016]
Nephelium lappaceum seed *biochar*	63.69	This study

3.8. Adsorption Mechanism

The primary mechanisms enabling CPX adsorption on BC are the hydrogen bond, hydrophobic, and electrostatic interactions depicted in Figure 9. The biochar surface's functional groups of the BC surface changed both before and after CPX adsorption, suggesting the participation of OH stretching, C=H stretching, and carbonyl C=O stretching. CPX's N-H functional groups can form hydrogen bonds with BC containing abundant oxygen, including C=O, -OH, and -COOH. The presence of these oxygen rich compounds in the BC was demonstrated by FTIR study. XRD analysis suggested changes in the crystal structure after adsorption. SEM-EDAX images confirmed the adsorption of cephalexin on the BC surface, with elemental analysis showing the presence of alumina and copper after adsorption. The point of zero charge (pHpzc) analysis indicated that the BC surface was positively charged at pH < 8.5 and negatively charged at pH > 8.5, making it effective for the electrostatic adsorption of CPX. Because of the electrostatic interaction, the charge on the surface of BC was induced by the pH of the sample interacting with the charged group in cephalexin. The aromatic ring portion of the CPX molecule can react with electrons in BC,

promoting π - π interaction and boosting adsorption. BC's surface has become more hydrophobic as oxygen-containing functional groups significantly influence the adsorption by providing specific sites for interactions, which results in the creation of hydrophobic interactions of BC that can attract the hydrophobic moieties in cephalexin to facilitate adsorption (Al Gheethi *et al.* 2021, Rashtbari *et al.* 2020).

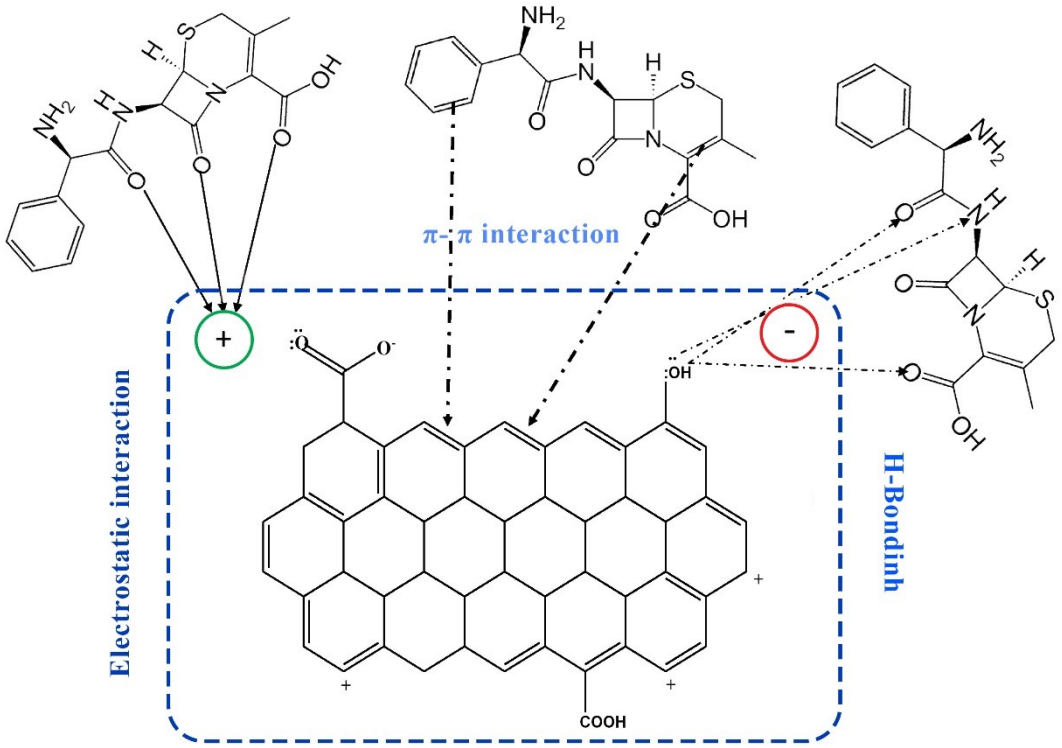

Figure 9. Mechanism of possible interaction between biochar and cephalexin.

4. CONCLUSIONS

The research evaluated using biochar produced from *Nephelium lappaceum* seeds to remove the widely used antibiotic cephalexin from an aqueous medium. FTIR, XRD, and SEM-EDAX were employed to evaluate the biochar before and after antibiotic adsorption. The impacts of different operating factors, namely pH, contact time, and cephalexin concentration, were examined with adsorption kinetics, isotherms, and thermodynamics. The maximum removal effectiveness was found at pH 6, with a temperature of 303.15 K, an adsorbent dose of 1.25 g/L, and an initial cephalexin concentration of 10-50 mg/L, with an

adsorption capacity of (63.69) mg/g. Based on kinetic investigations, the PSO model was more reliable with respect to the adsorption process, confirming a chemisorption mechanism. Thermodynamic analysis suggested that the adsorption process was feasible, spontaneous, and endothermic. Adsorption isotherm studies using Langmuir, Freundlich, and Temkin models exhibited good fits, with the Freundlich model having the highest R^2 value. This study provides insightful information regarding the prospective use of fruit seed-derived biochar for antibiotic removal, which will improve the development of effective and sustainable water treatment methods. Further research could focus on optimizing the conditions of BC production and exploring its uses in real-world water treatment scenarios. After further suitable improvement, cephalexin and perhaps other antibiotics could be removed from wastewater using this adsorbent.

REFERENCES

Acelas N., Lopera S.M., Porras J. and Torres-Palma R.A. (**2021),** Evaluating the removal of the antibiotic cephalexin from aqueous solutions using an adsorbent obtained from palm oil fiber, *Molecules*, **26,** 3340.

Adam O.E.A.A. (2016), Removal of resorcinol from aqueous solution by activated carbon: isotherms, thermodynamics and kinetics, *Journal of the American Chemical Society,* **16,** 1-13.

Ahmed M.J. and Theydan S.K. (2012), Adsorption of cephalexin onto activated carbons from Albizia lebbeck seed pods by microwave-induced KOH and K2CO3 activations. *Chemical engineering journal*, **211**, 200-207.

Al-Gheethi A., Noman E., Mohamed R.M.S.R., Talip B., Vo D.V.N. and Algaifi H.A. (2021), Cephalexin removal by a novel Cu–Zn bionanocomposite biosynthesized in secondary metabolic products of Aspergillus arenarioides EAN603 with pumpkin peels

medium: Optimization, kinetic and artificial neural network models, *Journal of Hazardous Materials*, **419**, 126500.

Al-Khalisy R.S., Al-Haidary A.M.A. and Al-Dujaili A.H. (2010), Aqueous phase adsorption of cephalexin onto bentonite and activated carbon, *Separation Science and Technology*, **45,**1286-1294.

Arab M., Faramarz M.G. and Hashim K. (2022), Applications of computational and statistical models for optimizing the electrochemical removal of cephalexin antibiotic from water, *Water*, **14**, 344.

Ashiq A., Sarkar B., Adassooriya N., Walpita J., Rajapaksha A.U., Ok Y.S. and Vithanage M. (2019), Sorption process of municipal solid waste biochar-montmorillonite composite for ciprofloxacin removal in aqueous media, *Chemosphere*, **236**, 124384.

Batool S., Shah A.A., Bakar A.F.A., Maah M.J. and Bakar N.K.A. (2022), Removal of organochlorine pesticides using zerovalent iron supported on biochar nanocomposite from Nephelium lappaceum (Rambutan) fruit peel waste, *Chemosphere*, **289**, 133011.

Chakraborty P., Banerjee S., Kumar S., Sadhukhan S. and Halder G. (2018), Elucidation of ibuprofen uptake capability of raw and steam activated biochar of Aegle marmelos shell: Isotherm, kinetics, thermodynamics and cost estimation, *Process Safety and Environmental Protection*, **118**, 10-23.

Dai Y., Li J. and Shan D. (2020), Adsorption of tetracycline in aqueous solution by biochar derived from waste Auricularia auricula dregs, *Chemosphere*, **238**, 124432.

Dehghan A., Zarei A., Jaafari J., Shams M. and Khaneghah, A.M. (2019), Tetracycline removal from aqueous solutions using zeoliticimidazolate frameworks with different morphologies: a mathematical modeling, *Chemosphere*, **217**,250-260.

Diaz-Uribe C., Walteros L., Duran F., Vallejo W. and Romero Bohórquez A.R. (2022), Prosopis juliflora Seed Waste as Biochar for the Removal of Blue Methylene: A Thermodynamic and Kinetic Study, *ACS omega*, **7**, 42916-42925.

Fan H.T., Shi L.Q., Shen H., Chen X. and Xie K.P. (2016), Equilibrium, isotherm, kinetic and thermodynamic studies for removal of tetracycline antibiotics by adsorption onto hazelnut shell derived activated carbons from aqueous media, *RSC advances*, **6**, 109983-109991.

Grisales-Cifuentes C.M., Galvis E.A.S., Porras J., Flórez E., Torres-Palma R.A. and Acelas N. (2021), Kinetics, isotherms, effect of structure, and computational analysis during the removal of three representative pharmaceuticals from water by adsorption using a biochar obtained from oil palm fiber, *Bioresource Technology*, **326**, 124753

Kandasamy S., Velusamy S., Thirumoorthy P., Periyasamy M., Senthilkumar V., Gopalakrishnan K.M., Sathish U., Kiramani V., Antrini F.D.G. and Periyasamy S. (2022), Adsorption of chromium ions from aqueous solutions by synthesized nanoparticles, *Journal of Nanomaterials*, 1-8.

Karthik V., Karuna B., Jeyanthi J. and Periyasamy S. (2023), Biochar production from *Manilkara zapota* seeds, activation and characterization for effective removal of Cu^{2+}ions in polluted drinking water, *Biomass Conversion and Biorefinery*, **13**, 9381-9395.

Karthik V., Mohanasundaram S., Ramaraju P., Jeyanthi J. and Periyasamy S.(2023), Study on the production, characterization, and application of coconut fiber biochar for effective removal of Co (II) ions from synthetic wastewater, *Biomass Conversion and Biorefinery*, **13**, 13677-13693

Karthik V., Selvakumar P., Sivarajasekar N., Megavarshini P., Brinda N., Kiruthika J., Balasubramani K., Ahamad T. and Naushad M. (2020), Comparative and equilibrium studies

554 on anionic and cationic dyes removal by nano-alumina-doped catechol formaldehyde
555 composite. *J Chemistry,* 1-15.
556 Khadem M., Husni Ibrahim A., Mokashi I., Hasan Fahmi A., NoemanTaqui S. Mohanavel
557 V., Hossain N., Baba Koki I., Elfasakhany A., Dhaif-Allah M.A. and Soudagar M.E.M.
558 (2023), Removal of heavy metals from wastewater using low-cost biochar prepared from
559 jackfruit seed waste. *Biomass Conversion and Biorefinery*, **13**, 14447-14456.
560 Li J., Yu G., Pan L., Li C., You F., Xie S., Wang Y., Ma J. and Shang X. (2018),Study of
561 ciprofloxacin removal by biochar obtained from used tea leaves, *Journal of Environmental*
562 *Sciences*, **73**, 20-30.
563 Liu H., Liu W., Zhang J., Zhang C., Ren L. and Li Y.(2011), Removal of cephalexin from
564 aqueous solutions by original and Cu (II)/Fe (III) impregnated activated carbons developed
565 from lotus stalks Kinetics and equilibrium studies, *Journal of hazardous materials*, **185,**
566 1528-1535.
567 Liu X., Sun J., Duan S.X., Wang Y.N., Hayat T., Alsaedi A., Wang C.M. and Li J.X. (2017),
568 A valuable biochar from poplar catkins with high adsorption capacity for both organic
569 pollutants and inorganic heavy metal ions, *Scientific Reports*, **7**, 10033.
570 Ma Y., Li P., Yang L., W, L., He L., Gao F. Qi X. and Zhang Z. (2020), Iron/zinc and
571 phosphoric acid modified sludge biochar as an efficient adsorbent for fluoroquinolones
572 antibiotics removal, *Ecotoxicology and Environmental Safety*, **2022196**, 110550.
573 Martins A.C., Pezoti O., Cazetta A.L., Bedin K.C., Yamazaki D.A., Bandoch G.F., Asefa T.,
574 Visentainer J.V. and Almeida V.C. (2015), Removal of tetracycline by NaOH-activated
575 carbon produced from macadamia nut shells: kinetic and equilibrium studies, *Journal of*
576 *Chemical & Engineering Data*, **260**, 291-299.

Miao M.S., Liu Q., Shu L., Wang Z., Liu Y.Z. and Kong Q. (2016), Removal of cephalexin from effluent by activated carbon prepared from alligator weed: Kinetics, isotherms, and thermodynamic analyses, *Process Safety and Environmental Protection*, **104**, 481-489.

Mondal N.K. and Kar S. (2018), Potentiality of banana peel for removal of Congo red dye from aqueous solution: isotherm, kinetics and thermodynamics studies, *Applied Water Science*, **8**, 1-12.

Naveen S. and Muthumari P. (2024), Synergistic Valorisation of Fruit and Vegetable Waste for Bioenergy Production: A Review, *International Research Journal of Multidisciplinary. Technovation*, 6, 61-79.

Periyasamy S., Karthik V., Senthil Kumar P., Isabel J.B., Temesgen T., Hunegnaw B.M., Melese B.B., Mohasmed B.A. and Vo D.V.N. (2022),Chemical, physical and biological methods to convert lignocellulosic waste into value-added products. A review, *Environmental Chemistry Letters,* **20**, 1129-1152.

Pezoti Jr O., Cazetta A.L., Souza I.P., Bedin K.C., Martins A.C., Silva T.L. and Almeida V.C. (2014), Adsorption studies of methylene blue onto ZnCl2-activated carbon produced from buriti shells (Mauritia flexuosa L.), *Journal of Industrial and Engineering Chemistry*, **20**, 4401-4407.

Phoon B.L., Ong C.C., Saheed M.S.M., Show P.L., Chang J.S., Ling T.C., Lam S.S. and Juan J.C. (2020),Conventional and emerging technologies for removal of antibiotics from wastewater, *Journal of Hazardous Materials*, **400,** 122961.

Priyadharsini P., SundarRajan P., Pavithra K.G., Naveen S., SanjayKumar S., Gnanaprakash D., Arun J. and Pugazhendhi A. (2023), Nanohybrid photocatalysts in dye (Colorants) wastewater treatment: Recent trends in simultaneous dye degradation, hydrogen production, storage and transport feasibility, *Journal of Cleaner Production*, 139180.

Rashtbari Y., Hazrati S., Azari A., Afshin S., Fazlzadeh M. and Vosoughi M. (2020), A novel, eco-friendly and green synthesis of PPAC-ZnO and PPAC-nZVI nanocomposite using pomegranate peel: Cephalexin adsorption experiments, mechanisms, isotherms and kinetics, *Advanced Powder Technology*, **31**, 1612-1623.

Samarghandi M.R., Al-Musawi T.J., Mohseni-Bandpi A. and Zarrabi M. (2015), Adsorption of cephalexin from aqueous solution using natural zeolite and zeolite coated with manganese oxide nanoparticles, *Journal of molecular liquids*, **211**,431-441.

Shirani Z., Song H. and Bhatnagar A. (2020), Efficient removal of diclofenac and cephalexin from aqueous solution using Anthriscussylvestris-derived activated biochar, *Science of the total environment*, **745**,140789.

Sun Y., Li H., Li G., Gao B., Yue Q. and Li X. **(**2016), Characterization and ciprofloxacin adsorption properties of activated carbons prepared from biomass wastes by H3PO4 activation, *Bioresource Technology*, **217**, 239-244.

Tang L., Yu J., Pang Y., Zeng G., Deng Y., Wang J., Ren X., Ye S., Peng B. and Feng H. (2018),Sustainable efficient adsorbent: alkali-acid modified magnetic biochar derived from sewage sludge for aqueous organic contaminant removal, *Journal of Chemical & Engineering*, **336**, 160-169.

Topal M. and Topal E.I.A. (2020), Optimization of tetracycline removal with chitosan obtained from mussel shells using RSM, *Journal of Industrial and Engineering Chemistry*, **84**, 315-321.

Varma V.C., Rathinam R., Suresh, V., Naveen S., Satishkumar P., Abdulrahman I.S., Salman H.M., Singh P. and Kumar J.A. (2024), Urban waste water management paradigm evolution: Decentralization, resource recovery, and water reclamation and reuse. *Environmental Quality Management*, **33**, 523-540.

625 Velusamy K., Periyasamy S., Kumar P.S., Jayaraj T., Krishnasamy R., Sindhu J., Sneka D.,
626 Subhashini B. and Vo D.V.N. (2021), Analysis on the removal of emerging contaminant from
627 aqueous solution using biochar derived from soap nut seeds, *Environmental Pollution*, **287**,
628 117632.
629 Venkateswaran N., Subbaiyan N., Punniyakotti Varadharajan G., Vellingiri S., Asary A.R.,
630 Giri J.M. and Petchimuthu P. (2023), A comprehensive review of the energy efficiency on
631 nano coated fin and tube condenser, *Environmental Quality Management*, **33**, 293-301.
632 Wang B., Li H., Liu T. and Guo J. (2021), Enhanced removal of cephalexin and sulfadiazine
633 in nitrifying membrane-aerated biofilm reactors, *Chemosphere*, **263**, 128224.
634 Wang J. and Wang S. (2019), Preparation, modification and environmental application of
635 biochar: A review, *Journal of Cleaner Production*, **227**, 1002-1022.
636 Xu C.M., Kong L.Q., Gao H.F., Cheng X.Y. and Wang X. M. (2022), A review of current
637 bacterial resistance to antibiotics in food animals, *Frontiers in Microbiology*, **13**, 822689.
638 Zhang X., Chu Y., Zhang H., Hu J., Wu F., Wu X., Shen G., Yang Y., Wang B. and Wang X.
639 (2021), A mechanistic study on removal efficiency of four antibiotics by animal and plant
640 origin precursors-derived biochars, *Science of the Total Environment*, **772,** 145468.